J|A|C|S
COMMUNICATIONS

Published on Web 08/08/2006

Doubly Ortho-Linked Quinoxaline/Diphenylfluorene Hybrids as Bipolar, Fluorescent Chameleons for Optoelectronic Applications

Chien-Tien Chen,*,† Yi Wei,† Jin-Sheng Lin,† Murthy V. R. K. Moturu,† Wei-San Chao,† Yu-Tai Tao,‡ and Chin-Hsiung Chien‡

Department of Chemistry, National Taiwan Normal University, and Institute of Chemistry, Academia Sinica, Taipei, Taiwan

Received April 17, 2006; E-mail: chefv043@ntnu.edu.tw

There has been great interest in the development of new electroluminescent molecular materials for organic light emitting diodes (OLEDs) in flat-panel display.[1a,b] In the aspect of advanced designs, integrating electron-transporting (ET) and hole-transporting (HT) segments into molecular materials may effectively improve the OLED device performance because of more balanced charge transports of both carriers.[1c] Several linearly D−A conjugated templates based on this concept[2−5] and attempts on single-layered devices[6] have thus been examined with significant success. Recently, we unraveled the first attempt of using doubly ortho-linked quinoxaline/triarylamine 1:1 hybrid as a bifunctional, dipolar electroluminescent clip for bluish green and orange OLED applications.[7] As part of our ongoing program on the use of dibenzosuberene (DBE)-based triarylcarbenium ions and over-crowded triarylethenes in catalysis[8] and LC optical switches,[9] we thought to merge the DBE template with fused quinoxaline backbones of varying electronic attributes for optoelectronic applications. In addition, to improve the rigidity, redox stability, and morphology of the DBE template, spiro-fluorene[10] is incorporated at the C5-position of the DBE template. Conceptually, the new molecular design connects the individual ortho-position of two phenyl rings in a HT-type 9,9-diphenylfluorene framework to the C2−C3 edge of a functionalized ET-type quinoxaline. Therefore, the resultant 1:1 hybrid is potentially bipolar and may act as a central fluorescent chameleon unit with tunable emission colors by judicious choices of the C5- and C8-appendages. Herein, we report the preliminary results toward this end with good to excellent optoelectronic performance in OLED applications (Scheme 1).

The starting **2**, derived from DBE-**1**, was oxidized by benzeneseleninic anhydride (BSA) to give diketone-**3** in 87% yield. Condensation of **3** and 3,6-dibromo-1,2-diaminobenzene with catalytic *p*-TSA in refluxed $CHCl_3$ provided quinoxaline-fused DBE-**4** in 90% yield. Attachments of respective aryl and arylamino components to both the C5 and C8 positions of the quinoxaline backbone in **4** were achieved by Suzuki and Hartwig coupling reactions, leading to **5a**−**d**, respectively in 70−95% yields.

The structural features for **5a**−**d** were resolved by NMR spectroscopy and ultimately proven by X-ray crystallographic analyses. For the aryl-conjugated systems **5a**−**c**, they share common structural attributes. They exist as a dimmer in unit cell. The flanking aryl appendages at both the C5 and C8 positions in the quinoxaline backbone are turned by 45−56° to avoid epi-interaction with the quinoxaline nitrogen lone pairs and steric interaction with the spirofluorene unit in another molecule (Figure 1a). The spirofluorene prevents facile conformational flipping of the central seven-memberd ring in the DBE core. Conversely, only one flanking nitrogen lone pair of the methylphenylamino groups in **5d** is somewhat coplanar (i.e., conjugated) with the quinoxaline backbone (Figure 1b). Nevertheless, resonance conjugations between the pendant aryl (or phenylamino) group and the quinoxaline backbone are prominent in solution, exerting progressive, bathochromic shifts in their UV and photoluminescence spectra, Table 1.

Upon UV excitation, these materials show different emission colors in solution varying from bluish, to green, to orange, to red. The full-width at half-maximum (fwhm) for each individual emission also increases progressively from 74, to 89, to 95, to 110 nm (Table 1), with quantum yields ranging from 34 to 78%. The increased molecular size and rigidity arising from the spiral framework of these materials are manifested in their increased thermal stability (T_d, 333−412 °C) and glassy transition temperature

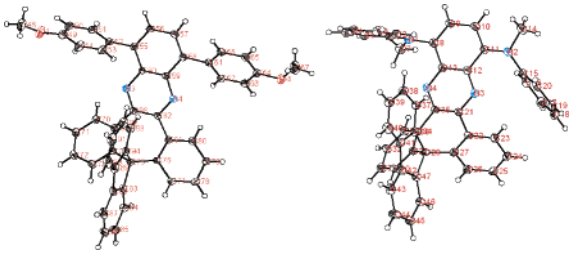

Figure 1. ORTEP diagram for X-ray crystal structure (ellipsoids are shown at 20% probability level) of (a) **5b** (left) and (b) **5d** (right).

Scheme 1. Assembly Concept of the Quinoxaline/Diphenylfluorene Optoelectronic System

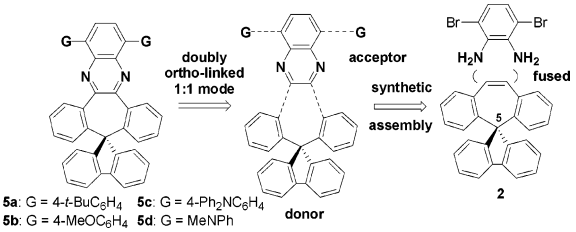

Table 1. Optical, Morphological, and CV Data for **5a**−**d** and **6**

compd	absorbance λ_{max} (ϵ)[a]	Em λ_{max}[a,b] nm	Φ_f[a] %	T_g/T_d °C	E_{red}/E_{ox}[a] V
5a	276 (63.8), 367 (17.2)	482 (74)	41	181/395	−2.07/- - -
5b	288 (60.6), 374 (15.7)	521 (89)	78	160/372	−2.07/- - -
5c	323 (17.4), 441 (3.6)	599 (95)	34	186/412	−2.05/+0.46
5d	332 (23.0), 482 (2.7)	650 (110)	42	153/333	−2.11/+0.08, +0.27
6	284 (58.9), 365 (17.6)	497 (97)	57	74 /321	−2.07/- - -

[a] λ_{max}, in nm; (ϵ) × 10^{-3}; measured in CH_2Cl_2. [b] The data in parentheses correspond to full-width at half-maximum (fwhm).

† National Taiwan Normal University.
‡ Academia Sinica.

10.1021/ja062660v CCC: $33.50

Table 2. Electroluminescence Data for **5a**−**d** and **6**

conf[a]	Em[b] λ_{max}	V_{on}[c] V	η_{ext}[c]	η_c/η_p[c]	L[c] cd/m^2
5a/A	490 (70)	4.5 (4.9)	0.45	0.82/0.52	5995 (205)
5b/A	520 (82)	2.5 (4.0)	1.92	6.35/5.02	35372 (1268)
5b/B	524 (88)	4.7 (7.4)	1.06	2.90/1.19	11733 (414)
6/A	502 (90)	2.7 (4.0)	1.75	5.07/3.95	20640 (1055)
Alq_3/A	516(104)	3.9 (5.6)	1.11	3.29/1.84	28911 (638)
5c/A	576 (95)	2.8 (3.9)	0.98	2.54/2.05	23716 (524)
5c/B	580 (97)	3.9 (6.5)	2.90	7.75/3.73	20683 (1542)
5c/C	578 (96)	4.4 (6.3)	4.92	13.10/6.54	69700 (2503)
5d/A	642(102)	3.7 (5.7)	0.81	0.85/0.47	3558 (167)
5d/B	644(101)	4.1 (5.8)	3.17	2.31/1.21	11484 (1102)

[a] Configuration (conf) **A:** ITO/NPB (40 nm)/**5a**−**d** (40 nm)/LiF (1 nm)/Al; **B:** ITO/**5b**−**d** (40 nm)/BCP (10 nm)/Alq_3 (40 nm)/LiF (1 nm)/Al; **C:** ITO/NPB (40 nm)/**5c** (40 nm)/BCP (10 nm)/Alq_3 (40 nm)/LiF (1 nm)/Al. [b] The data in parentheses correspond to full-width at half-maximum (fwhm). [c] The data in parentheses for V_{on} and L and the data for η_{ext} (%), η_c (cd/A), and η_p (lm/W) were measured at 20 mA/cm^2.

(T_g, 153−186 °C). For example, the T_d and T_g (372 °C and 160 °C) for **5b** ($C_{47}H_{32}N_2O_2$, fw: 656.8) are 51 and 86 °C higher than those (321 °C and 74 °C) for the corresponding open-form system-**6** [i.e., 5,8-bis-(4-methoxyphenyl)-2,3-diphenyl-quinoxaline ($C_{34}H_{26}N_2O_2$, fw: 494.6)].

The redox behaviors of **5a**−**d** were evaluated by cyclic voltammetry (CV) experiments at ambient temperature. They exhibit similar reduction potentials with reversible redox couples at −2.08 ± 0.03 V. No discernible oxidations were found in less than +1.5 V for **5a** and **5b**. Nevertheless, reversible two-electron oxidation redox couples can be identified for triarylamino-containing **5c** and **5d**. They show oxidation potential at +0.46 V for **5c** and a pair of +0.08 and +0.27 eV for **5d** owing to sequential oxidations of the two amino appendages. When compared with Ar_3N/quinoxaline[4a,b] and spiro-fluorene-based dipolar hybrids,[5d] the current new designs show slightly lower redox potentials, which may facilitate better charge injection from both carriers.

Their optoelectronic performances are evaluated as respective ET-type and HT-type emitting layers by fabricating bilayer or trilayer OLED devices with two different configurations. 1,4-Bis-(1-naphthylphenylamino)-biphenyl (α-NPB[11]) and Alq_3 were employed (40 nm thickness each) as HT and ET layers, respectively. In the combination of respective **5a**−**d** with Alq_3, 2,9-dimethyl-4,7-diphenyl-1,10-phenanthroline (BCP) was utilized as a hole blocking layer (10 nm) to completely suppress emission leakage from Alq_3. When **5a**, **5b**, **5c**, and **5d** were examined as ET and emitting materials in device configuration A (Table 2), the resultant OLED devices exhibit maximum EL brightness (L_{max}) of 5995, 35372, 23716, and 3558 cd/m^2, respectively. Their operational brightness (L_{20}) at 20 mA/cm^2 can reach 205, 1268, 524, and 167 cd/m^2, respectively, with individual external quantum efficiency (η_{ext}) of 0.5, 1.9, 1.0, and 0.8%. Their luminance and power efficiencies (η_c/η_p) are 0.8/0.5, 6.4/5.0, 2.5/2.1, and 0.9/0.5 cd A^{-1}/lm W^{-1}, respectively. Notably, **5b** acted more as a superior ET and emitting dipolar material than Alq_3 in terms of operational voltage (4.0 vs 5.6 V), emission peak width (fwhm: 82 vs 104 nm), L_{20} (12688 vs 638 cd/m^2), η_{ext} (1.9 vs 1.1%), and working efficiencies (6.4/5.0 vs 3.3/1.8 cd A^{-1}/lm W^{-1}) when both devices were fabricated simultaneously under the same conditions.

Conversely, when **5a**−**d** were examined as HT and emitting materials in device configuration B (Table 2), all the devices except that from **5a** showed promising results. The resultant OLED devices from **5b**, **5c**, and **5d** exhibit a maximum EL brightness (L_{max}) of 11773, 20683, and 11484 cd/m^2, respectively. Their operational brightness (L_{20}) at 20 mA/cm^2 can reach 414, 1542, and 1102 cd/m^2, respectively, with individual external quantum efficiency (η_{ext}) of 1.1, 2.9, and 3.2%. Their respective luminance and power efficiencies (η_c/η_p) are 2.9/1.2, 7.8/3.7, and 2.3/1.2 cd A^{-1}/lm W^{-1}.

Overall, the optoelectronic performance is 2 times better when **5b** is utilized as an ET and emitting layer. On the contrary, the optoelectronic performances are 2−3 times better when **5c** or **5d** is employed as HT and emitting layers. Nevertheless, both the **5b** and **5c** can function as bipolar electroluminescent materials with more balanced charge transporting properties in view of the satisfactory OLED performances in complementary device configurations A and B. To further optimize the device efficiency, we have also fabricated a four-layered device with a configuration of α-NPB/**5c** (40 nm)/BCP/Alq_3 (configuration C). For this combination of using **5c** as the sole emitting layer, the OLED device exhibits L_{max} and L_{20} of 69700 and 2503 cd/m^2 with η_{ext} of 4.9%. The luminance and power efficiencies (η_c/η_p) are 13.1/6.5 cd A^{-1}/lm W^{-1}. To our knowledge, green emitting **5b**, yellow-emitting **5c**, and red emitting **5d** represent one of the best bipolar fluorescent materials to date.[12]

Acknowledgment. We thank the National Science Council of Taiwan for generous financial support of this research.

Supporting Information Available: Experimental, device, and spectra details of **2**−**6** and cif files for **5b** and **5d**. This material is available free of charge via the Internet at http://pubs.acs.org.

References

(1) (a) Hung, L. S.; Chen, C. H. *Mater. Sci. Eng. Report* **2002**, 39, 143. (b) Burroughes, J. H.; Bradley, D. D. C.; Brown, A. R.; Marks, R. N.; Mackay, K.; Friend, R. H.; Burns, P. L.; Holmes, A. B. *Nature* **1990**, *347*, 539. (c) Mullen, K.; Scherf, U. *Organic Light-Emitting Devices. Synthesis, Properties and Applications*; Wiley: Weinheim, Germany, 2006.

(2) (a) Mochizuki, H.; Hasui, T.; Kawamoto, M.; Shiono, T.; Ikeda, T.; Adachi, C.; Taniguchi, Y.; Shirota, Y. *Chem. Commun.* **2000**, 1923. (b) Tamoto, N.; Adachi, C.; Nagai, K. *Chem. Mater.* **1997**, *9*, 1077. (c) Peng, Z. H.; Bao, Z. N.; Galvin, M. E. *Chem. Mater.* **1998**, *10*, 2086.

(3) (a) Liu, Y.; Ma, H.; Jen, A. K.-Y. *Chem. Commun.* **1998**, 2747. (b) Wang, Y. Z.; Epstein, A. J. *Acc. Chem. Res.* **1999**, *32*, 217. (c) Jenekhe, S. A.; Lu, L. D.; Alam, M. M. *Macromolecules* **2001**, *34*, 7315.

(4) (a) Justin Thomas, K. R.; Lin, J. T.; Tao, Y.-T.; Chuen, C.-H. *Chem. Mater.* **2002**, *14*, 3852. (b) Kido, J.; Harada, G.; Nagai, K. *Chem. Lett.* **1996**, 161. (c) Song, S.-Y.; Jang, M. S.; Shim, H.-K.; Hwang, D.-H.; Zyung, T. *Macromolecules* **1999**, *32*, 1482. (d) For quinoxaline-thiophene alternating polymers, see the following: Nurulla, I.; Yamaguchi, I.; Yamamoto, T. *Polym. Bull.* **2000**, *44*, 231. (e) Yamamoto, T.; Zhou, Z.-H.; Kanbara, T.; Shimura, M.; Kizu, K.; Maruyama, T.; Nakamura, Y.; Fukuda, T.; Lee, B.-L.; Ooba, N.; Tomaru, S.; Kurihara, T.; Kaino, T.; Kubota, K.; Sasaki, S. *J. Am. Chem. Soc.* **1996**, *118*, 10389.

(5) (a) Geng, Y.; Katsis, D.; Culligan, S. W.; Ou, J. J.; Chen, S. H.; Rothberg, L. J. *Chem. Mater.* **2002**, *14*, 463. (b) Wong, K.-T.; Chien, Y.-Y.; Chen, R.-T.; Wang, C.-F.; Lin, Y.-T.; Chiang, H.-H.; Hsieh, P.-Y.; Wu, C.-C.; Chou, C. H.; Su, Y. O.; Lee, G.-H.; Peng, S.-M. *J. Am. Chem. Soc.* **2002**, *124*, 11576. (c) Wong, K.-T.; Hwu, T.-Y.; Balaiah, A.; Chao, T.-C.; Fang, F.-C.; Lee, C.-T.; Peng, Y.-C. *Org. Lett.* **2006**, *8*, 1415. (d) Fungo, F.; Wong, K.-T.; Ku, S.-Y.; Hung, Y.-Y.; Bard, A. J. *J. Phys. Chem. B.* **2005**, *109*, 3984.

(6) (a) Zhu, W.; Hu, M.; Yao, R.; Tian, H. *J. Photochem. Photobiol., A* **2003**, *154*, 109. (b) Freudenmann, R.; Behnisch, B.; Hanack, M. *J. Mater. Chem.* **2001**, *11*, 1618. (c) Hassheider, T.; Benning, S. A.; Kitzerow, M. F.; Bock, A. H. *Angew. Chem., Int. Ed.* **2001**, *40*, 2060.

(7) Chen, C.-T.; Lin, J.-S.; Moturu, M. V. R. K.; Lin, Y.-W.; Yi, W.; Tao, Y.-T.; Chien, C.-H. *Chem. Commun.* **2005**, 3980.

(8) Chen, C.-T.; Chao, S.-D.; Yen, K.-C.; Chen, C.-H.; Chou, I.-C.; Hon, S.-W. *J. Am. Chem. Soc.* **1997**, *119*, 11341.

(9) Chen, C.-T.; Chou, Y.-C. *J. Am. Chem. Soc.* **2000**, *122*, 7662

(10) (a) Chien, Y.-Y.; Wong, K.-T.; Chou, P.-T.; Cheng, Y.-M. *Chem. Commun.* **2002**, 2874. (b) Wong, K.-T.; Chen, R.-T.; Fang, F.-C.; Wu, C.-C.; Lin, Y.-T. *Org. Lett.* **2005**, *7*, 1979.

(11) (a) Koene, B. E.; Loy, D. E.; Thompson, M. E. *Chem. Mater.* **1998**, *10*, 2235. (b) O'Brien, D. F.; Burrows, P. E.; Forrest, S. R.; Koene, B. E.; Loy, D. E.; Thompson, M. E. *Adv. Mater.* **1998**, *10*, 1108.

(12) (a) Huang, T.-H.; Lin, J.-T.; Chen, L.-Y.; Lin, Y.-T.; Wu, C.-C. *Adv. Mater.* 2006, *18*, 602. (b) Justin Thomas, K. R.; Lin, J. T.; Tao, Y.-T.; Chuen, C.-H. *Chem. Mater.* **2002**, *14*, 2796. (b) Chen, C.-T. *Chem. Mater.* **2004**, *16*, 4389.

JA062660V